PAPER

Catalytic hydrogenation of dihydrolevoglucosenone to levoglucosanol with a hydrotalcite/mixed oxide copper catalyst†

Mario De bruyn, [ID] *[a,b] Canan Sener, [ID] [a] Davi D. Petrolini, [ID] [c] Daniel J. McClelland, [ID] [a,d] Jiayue He, [ID] [a] Madelyn R. Ball, [ID] [a] Yifei Liu,[a] Leandro Martins, [ID] [c] James A. Dumesic, [ID] [a] George W. Huber [ID] [a] and Bert M. Weckhuysen [ID] [b]

Levoglucosanol (LGOL) is a critical intermediate for the bio-based production of hexane-1,2,5,6-tetrol, 1,2,6-hexanetriol, and 1,6-hexanediol. Here we report on the aqueous-phase hydrogenation of cellulose-derived dihydrolevoglucosenone (Cyrene™) to LGOL using a calcined and reduced heterogeneous copper/hydrotalcite/mixed oxide catalyst, denoted as Cu8/MgAlO$_x$-**HP**. The turnover frequency for LGOL conversion over this copper-containing catalyst is equal to 0.013 s^{-1} at 353 K as measured in a flow reactor which is half the one obtained using 0.4 wt% Pd/Al$_2$O$_3$. Moreover, while Cu8/MgAlO$_x$-**HP** shows a stable activity, the activity of 0.4 wt% Pd/Al$_2$O$_3$ decreases with time-on-stream. Neither Cu- nor Al-leaching is observed (resp. <1 ppb and <1 ppm) but Mg leaching can be seen (5.5 ppm). The latter leaching relates to the acidity of the Cyrene/H$_2$O mixture (pH 3.5–4.5 range), which is due to the occurrence of the geminal diol moiety of Cyrene, an acidic species. In contrast, additional and consecutive oxidation and reduction of the catalyst leads to a gradual decrease in activity over time. Applying still further oxidation/reduction cycles to this catalyst tends to decrease its activity with some overall stabilization being observed from the fourth run onwards. Mg-leaching is shown to change the relative meso-to-macro pore content, but leaves the total pore volume unchanged between the fresh and the spent catalyst. In spite of the high copper loading (8 wt%), small Cu-nanoparticles (2–3 nm) are present over the hydrotalcite/mixed oxide surface of the Cu8/MgAlO$_x$-**HP** material, and these particles do not aggregate during the hydrogenation reaction.

Introduction

Heterogeneous catalysis has been a longstanding and pivotal technology for the conversion of petrochemical feedstocks into fuels and chemicals, and more recently also for the conversion of biomass.[1–4] To date, Group VIII metals have been extensively relied upon, most notably Pt, Pd and Rh. However, these metals are costly and pose critical future supply issues.[5] Thus, significant attention has been devoted to the development of base

[a]*Department of chemical and biological engineering, University of Wisconsin-Madison, 1415 Engineering Drive, 53706 Wisconsin, USA. E-mail: debruyn@wisc.edu, mario.debruyn@gmail.com*
[b]*Faculty of Science, Debye Institute for Nanomaterials Science, Utrecht University, Universiteitsweg 99, CGUtrecht 3584, The Netherlands*
[c]*Instituto de Química, Unesp - Universidade Estadual Paulista, R. Prof. Francisco Degni 55, CEP 14800-900 Araraquara, SP, Brazil*
[d]*DOE Center for Advanced Bioenergy and Bioproducts Innovation, University of Wisconsin-Madison, 1415 Engineering Drive, 53706 Wisconsin, USA*
†Electronic supplementary information (ESI) available. See DOI: 10.1039/ c9gc00564a

metal catalysts, most commonly Fe, Cu, Ni and Co. The use of these elements is not always straightforward; for instance, both Ni and Co are suspect carcinogenics.[6,7] Also, when used as heterogeneous catalysts in polar media, such as water, these metals tend to leach.[8] The specific case of cobalt is even more problematic as (1) it is an essential component in Li-ion batteries making for a current demand in excess of 100 000 metric tons at a compound annual growth rate (CAGR) of 11.6% and (2) no less than 2/3 of the world's cobalt supply is mined in the Democratic Republic of Congo.[9] In marked contrast, copper is only of medium economic importance and has a reduced supply risk.[5]

Supported copper catalysts have been reported for the reduction of both C–C double/triple bonds and a range of carbonyl groups, with CuCrO$_4$ and Cu/ZnO being common.[10,11] However, as Cu-based solid catalysts tend to suffer poor stability, the addition of earth alkaline oxides or Al$_2$O$_3$ is often needed to prevent metal sintering.[12] This lack of stability is of particular importance in gas-phase reactions where the applied reaction temperature can exceed 410 K *i.e.* the temperature at which surface Cu-atoms become mobile.[11] Organic

liquid phase (transfer) hydrogenation reactions of carbonyl groups using supported Cu catalysts have also been reported.[13–15] Few successful aqueous hydrogenations using supported Cu-catalysts are documented; a rare example is the reduction of furfural to furfuryl alcohol in water with a 5 wt% Cu/Al_2O_3 (90 °C, 20 bar H_2) catalyst, yielding 81% furfuryl alcohol at 81% conversion.[16]

Here we report on an active Cu/hydrotalcite/mixed oxide catalyst that does not show measureable leaching of Cu during the low temperature H_2-mediated hydrogenation of dihydrolevoglucosenone (Cyrene™) to *exo* and *endo* levoglucosanol (LGOL) in water (Scheme 1). Irrespective of the catalyst pretreatment, neither copper (<ppb) nor aluminium (<1 ppm) leaching could be observed. In contrast, 9.5 ppm Mg-leaching was detected for calcined/reduced Cu8/MgAlO$_x$-**HP** and 5.5 ppm for only reduced Cu8/MgAlO$_x$-**HP**. This leaching of Mg could be linked to the dominant presence of the geminal diol nature of Cyrene, an acidic species formed by the reaction of

Cyrene with water. The reduced catalyst was found to yield a constant conversion (75%) over 25 h time-on-stream, while the performance of the oxidized/reduced catalyst decreased gradually, though eventually stabilizing. Batch operation is found more suitable to higher Cyrene concentrations than flow operation. This work on the conversion of Cyrene to LGOL reflects the growing interest in an alternative biorefinery concept where biomass-derived carbohydrates are directly converted to levoglucosenone (LGO) instead of mono/oligo carbohydrates and furan-containing molecules.[17–19] Indeed, clear synthetic routes from levoglucosanol (LGOL) (*i.e.*, fully hydrogenated LGO or Cyrene) to *cis/trans* tetrahydro-2,5-furan-dimethanol (THFDM); 1,2,6-hexanetriol (HTO) and 1,6-hexanediol (1,6-HDO) have been shown in publications by our group and a range of DuPont patents.[20–22] Furthermore, we have recently reported on the direct conversion of LGOL into (*S,R*)/(*S,S*) hexane-1,2,5,6-tetrol (1256HT), a versatile new bio-derived synthon, in high yield.[23] These molecules can be used in a range of industrial applications as outlined in Fig. 1.

Results and discussion

Batch reactions

The catalytic hydrogenation of Cyrene to LGOL was studied from 5 wt% Cyrene in water solutions and using 8 wt% (ICP) copper supported on a mesoporous/macroporous structured MgAl hydrotalcite (Mg/Al = 1) – hereafter this catalyst is denoted as Cu8/MgAlO$_x$-**HP**. The catalyst was always oxidized
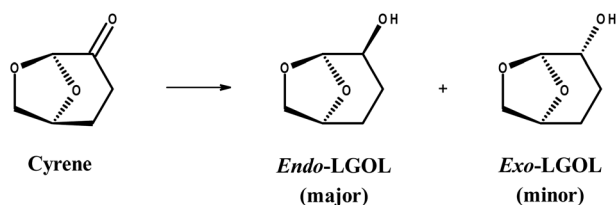
Scheme 1 Hydrogenation of dihydrolevoglucosenone (Cyrene™) into *endo/exo*-levoglucosanol (LGOL).
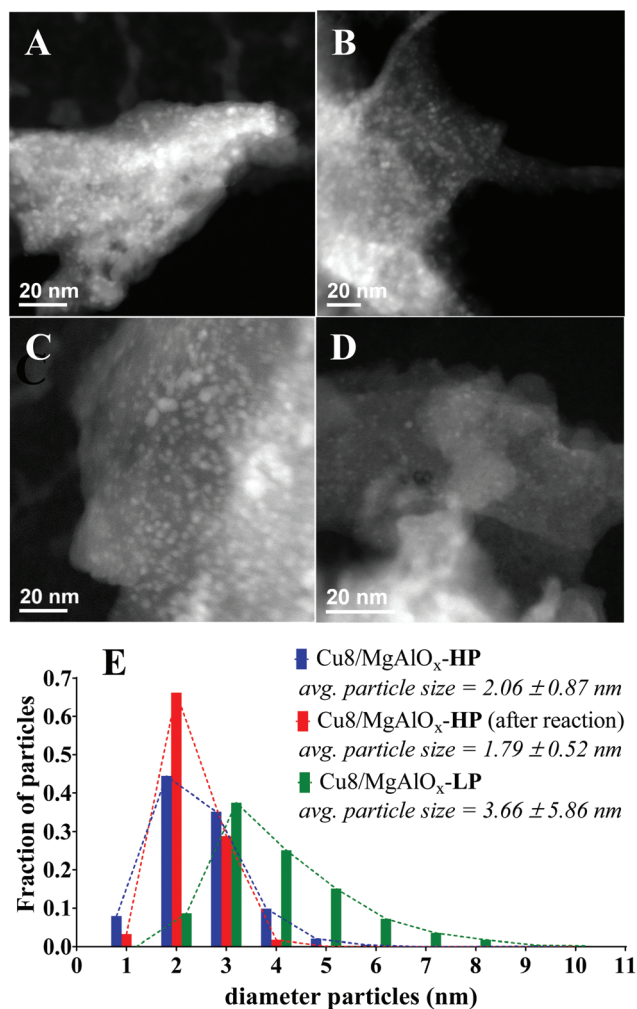

Fig. 1 Overview of the synthetic possibilities starting from levoglucosanol (LGOL) as a platform molecule.

and reduced and then further subjected to a re-reduction or additional oxidation/reduction cycles, as indicated. The hydrotalcite support was made following a recently published procedure by Petrolini *et al.* and constitutes the sol–gel transition of Mg and Al precursors in the presence of structure directing agents (SDA): pluronic surfactant and *n*-dodecane as an emulsion.[24] Using this catalyst, batch reactor experiments were conducted to explore the effect of hydrogen pressure on the hydrogenation of Cyrene to LGOL at a fixed temperature of 333 K and for a fixed reaction time of 18 h. The LGOL conversion increased with increasing hydrogen pressure, suggesting a positive reaction order in hydrogen (Fig. 2A). The LGOL *endo/exo* ratios were found to be insensitive to both hydrogen pressure and conversion. Cu8/MgAlO$_x$-**HP** had a higher activity than Cu8/MgAlO$_x$-**LP**, a reference catalyst prepared in the absence of SDA (Fig. 2A). This higher activity could be attributed to an enhanced copper dispersion on Cu8/MgAlO$_x$-**HP** than on its less porous equivalent Cu8/MgAlO$_x$-**LP** – respectively 7.2 *vs.* 5.3% (as determined by N$_2$O titration – see ESI† for details). In this respect, we note that MgAlO$_x$-**HP** and MgAlO$_x$-

Fig. 3 TEM images of Cu8/MgAlO$_x$-**HP** (A & B); Cu8/MgAlO$_x$-**LP** (C) and Cu8/MgAlO$_x$-**HP** after batch reaction (333 K for 18 h) (D); subfigure E depicts their respective Cu-nanoparticle size distributions. Average (avg.) particle sizes determined from ~1000 particles.

Fig. 2 (A) Effect of the H$_2$ pressure on the LGOL yield and its *endo/exo* ratio for the Cu8/MgAlO$_x$-**HP** and Cu8/MgAlO$_x$-**LP** catalysed Cyrene to LGOL conversion at 333 K for 18 h (B) influence of the temperature (353 & 373 K) on the Cyrene to LGOL reaction with the Cu8/MgAlO$_x$-**HP** catalyst. Batch reactor. All batch experiments were conducted with 2 mmol Cyrene in 5 mL water (~4.9 wt%), 25 mg catalyst and 60 bar H$_2$.

LP have respective surface areas of 171 and 106 m^2 g^{-1}. Furthermore, given the high copper loading of 8 wt%, it is also noteworthy that Cu deposition on the highly mesoporous MgAlO$_x$-**HP** gives a narrower particle size distribution (2–4 nm) than obtained for Cu8/MgAlO$_x$-**LP** (2–10 nm range) (Fig. 3). Importantly, the Cu-particle size distribution was found to be nearly identical before and after reaction (Fig. 3). In terms of the turnover frequency (TOF), Cu8MgAlO$_x$-**HP** and Cu8MgAlO$_x$-**LP** realize respective TOFs (333 K) of 0.0117 s^{-1} and 0.0093 s^{-1}, representing a 20% increase in activity. Cu 2p XPS analysis of oxidized/reduced Cu8/MgAlO$_x$-**HP** (Fig. 4A – Scan A) and Cu8/MgAlO$_x$-**LP** (Fig. 4A – Scan B) revealed the absence of Cu(II) species. Additional examination of the Auger LMM spectrum points to the presence of Cu(I) and Cu(0) in both Cu8/MgAlO$_x$-**LP** & **HP** (Fig. 4B – Scans A&B). Fig. 2B shows the influence of temperature (353 and 373 K) on the catalytic activity of Cu8/MgAlO$_x$-**HP** in Cyrene/LGOL hydrogenation. The TOF (~45% conversion) is 0.116 s^{-1} at 373 K. Table 1S† details the
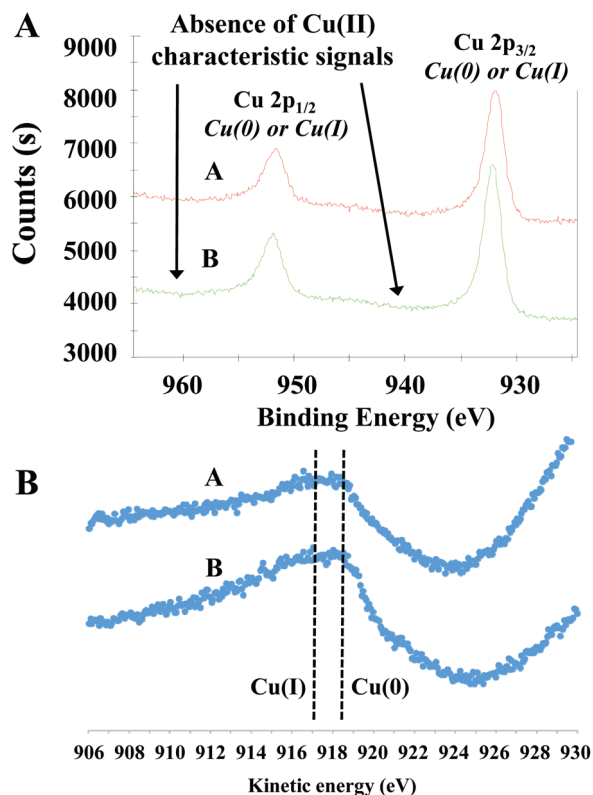
Fig. 4 (A) X-ray photoelectron spectroscopy (XPS) data of Cu8/MgAlO$_x$-**HP** (scan A) and Cu8/MgAlO$_x$-**LP** (scan B); (B) Auger LMM spectra of Cu8/MgAlO$_x$-**HP** (scan A) and Cu8/MgAlO$_x$-**LP** (scan B).

observed rates for a range of flow/batch reactions. The activation energy (E_a) was determined to be 59 kJ mol^{-1} over the 333–373 K temperature range.

Flow reactions

To evaluate further the performance of these Cu-based catalyst materials, flow experiments were performed. In a first approach, the performance of oxidized/reduced Cu8/MgAlO$_x$-**HP** was evaluated (Fig. 5A). A mild decrease of catalytic activity is observed for the first three runs, the first order deactivation rate constant being −0.0027 h^{-1}. The ICP analysis indicated that neither Cu nor Al leaching (respectively <1 ppb and <1 ppm) was occurring but rather, a consistent leaching of ~9.5 ppm Mg took place. Increasing the initial Cyrene concentration from 1 to 5 wt% was found to amplify the Mg-leaching to ~30 ppm with again no detectable loss of copper nor aluminium (Fig. 5B). It is noteworthy, however, that a five times increase of the Cyrene concentration gives a ten times higher decrease in the initial catalytic activity [to a value of 0.027 h^{-1}]. Following these observations, the pH of a range of Cyrene/H$_2$O solutions was measured, revealing a decrease of the pH even at Cyrene concentrations down to 1 wt% (Fig. 5C). This phenomenon can be attributed to the formation of geminal diol functionality of Cyrene,[25] a chemical species displaying at least one acidic hydroxyl group (Fig. 5D). This behaviour is reminiscent of the work by Delidovich *et al.* on hydrotalcite-catalyzed
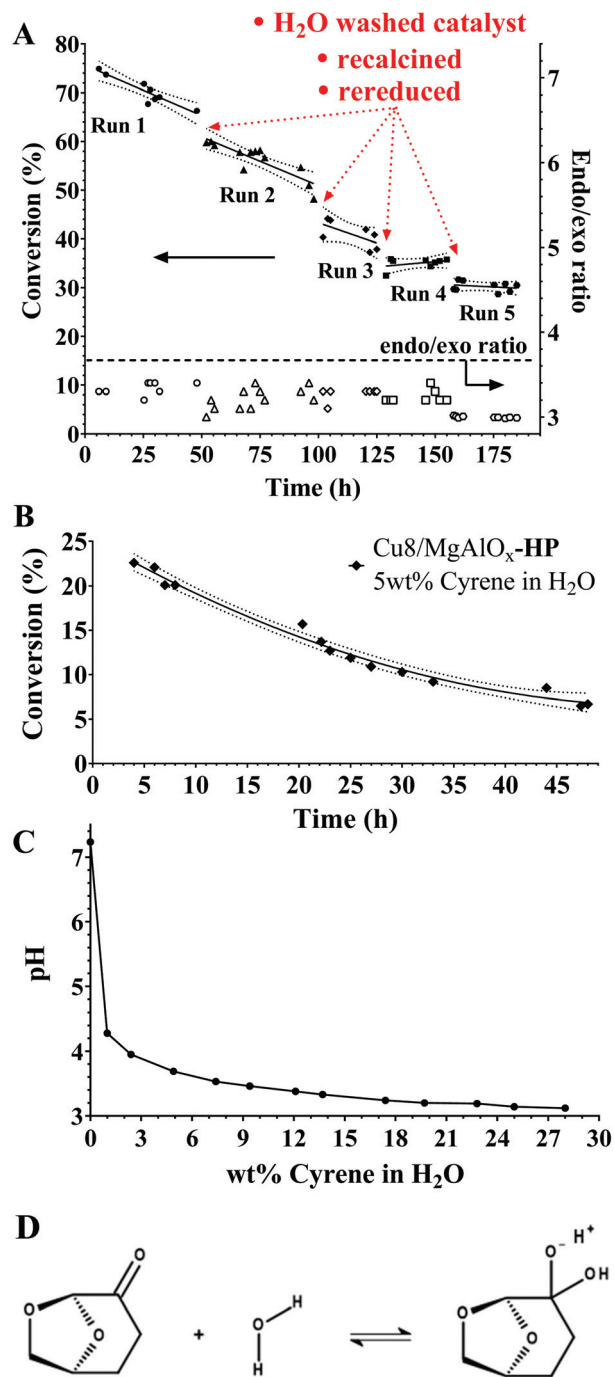

Fig. 5 (A) Five consecutive Cyrene to LGOL flow reactions (353 K, 60 bar H$_2$, 1 wt% Cyrene in H$_2$O) using 25 mg Cu8/MgAlO$_x$-**HP** as the catalyst; after each run the catalyst is re-oxidized and re-reduced (B) Cu8/MgAlO$_x$-**HP** catalysed Cyrene to LGOL reaction using a 5 wt% Cyrene in H$_2$O solution (353 K, 60 bar H$_2$) (C) pH of a range of Cyrene/H$_2$O mixtures as a function of the initial Cyrene concentration in wt%. (D) Scheme of the Cyrene hydration reaction. Flow conditions (A) and (B): Cyrene/H$_2$O solution: 0.03 mL min^{-1}, H$_2$ gas: 20 mL min^{-1}.

glucose-fructose isomerization, where the lactic acid side product is shown to leach Mg, and not Al, from the hydrotalcite catalyst without causing structural deformation of the catalyst.[26] The reasons for the mild decrease of catalytic

Table 1 Textural properties of the catalysts as determined by N_2 physisorption and mercury intrusion porosimetry

	Pore volume mL g^{-1}				
	Meso	Macro	Total	Micro pore *t*-plot	BET area m^2 g^{-1}
Cu8/MgAlOx-**LP**	0.2	0.3	0.5	0	106
Cu8/MgAlOx-**HP**	0.3	1.0	1.3	0	171
Cu8/MgAlOx-**HP** *after reaction*	0.4	0.9	1.3	0	60

activity during the flow experiments are presently unclear but may relate to the below options:

(1) Active Mg-leaching may undermine the stability of the hierarchical pore structure in the Cu8/MgAlOx-**HP** material. This change in pore structure could make active copper sites progressively unavailable for reaction hence the gradual decrease of the catalytic activity over time.

(2) Active Mg-leaching may create additional (micro) pores, potentially allowing non-copper-containing flow routes to the Cyrene/water reaction mixture.

(3) Even though no net copper leaching can be observed, it is possible that copper species leach locally yet rapidly form water insoluble species like Cu(ɪɪ) carbonate hydroxide. While the latter explanation is unlikely given the acidic reaction medium, one could envisage the gradual (partial) formation of copper aluminates, such as *copper aluminate spinel (CuAl$_2$O$_4$) or cuprous aluminate delafossite (CuAlO$_2$)*, during the reaction, a process known to require the presence of dilute acid.[27]

To evaluate hypothesis 1 & 2 we have performed N_2 physisorption and Hg intrusion porosimetry on Cu8/MgAlO$_x$-**HP**, Cu8/MgAlO$_x$-**LP** and "Cu8/MgAlO$_x$-**HP** after reaction" (Table 1 and Fig. S1 and S2†). From Table 1 it can be inferred that "Cu8/MgAlO$_x$-**HP** after reaction" has a somewhat increased mesopore content, which is however balanced by a slight decrease in the macropore content, leaving the total pore volume (meso + macro) equal between the fresh and the spent catalyst. We tentatively relate these changes in the relative meso- and macropore content to structural rearrangements of the pores, which may relate to Mg-leaching from the catalyst. No significant difference in pore size distribution (macro + meso) could be found between the fresh and the spent catalyst (Fig. 2S†). All determined isotherms are type IV and no (superimposed) type I isotherm can be inferred (Fig. 2S†); applying the *t*-plot to the determined isotherms shows no indication of the occurrence of micropores.

It is further noteworthy that the fourth and fifth runs depicted in Fig. 5A show an effective stabilization of the catalytic activity. TEM analysis of the catalyst before and after batch reaction shows no apparent changes in the particle size (distribution) of the Cu nanoparticles (Fig. 3B, D & E). This observation is in agreement with the ICP-established absence of Cu-leaching and also indicates that the Cu nanoparticles in this catalyst are not prone to agglomeration. XPS of the spent catalyst reveals the presence of Cu(ɪɪ) (Fig. 6A) although the
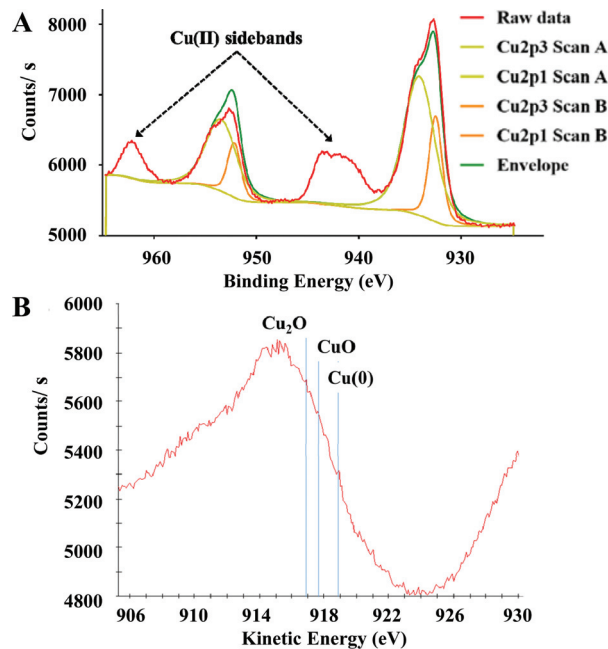
Fig. 6 (A) X-ray photoelectron spectroscopy (XPS) data of recovered Cu8/MgAlO$_x$-**HP** (with peak fitting) and (B) Auger LMM spectra of recovered Cu8/MgAlO$_x$-**HP**.

combined XPS/Auger spectra also hint at the presence of Cu(ɪ) (Fig. 6A/B). It was found that the stability of the catalyst material could be improved when, instead of dual oxidation/reduction, only a reduction step was applied (Fig. 7). This result hints at a negative influence of re-oxidation of the catalyst, its main function being the re-conversion of hydrotalcite into mixed oxide. For this reduced catalyst, ICP-AES analysis showed the absence of both Cu and Al-leaching, while Mg-leaching was found to decrease to 5.5 ppm. This result implies that the reduced Cu8/MgAlO$_x$-**HP** may be more stable than oxidized/reduced Cu8/MgAlO$_x$-**HP**. In flow reactor studies, reduced Cu8/MgAlO$_x$-**HP** was found to maintain constant activity with an increase of the Cyrene concentration in the
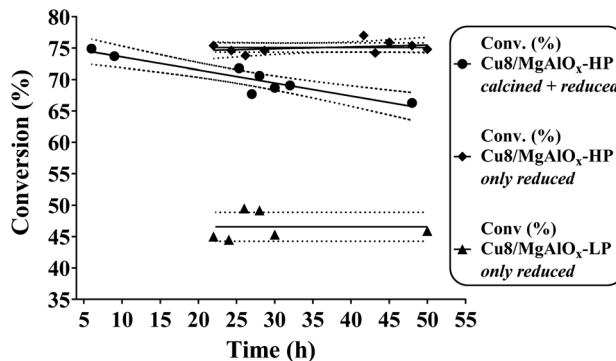
Fig. 7 Comparative activity of "oxidized and reduced" and "sole reduced" Cu8/MgAlO$_x$-**HP** in flow (353 K, 60 bar H$_2$, 1 wt% Cyrene in H$_2$O). Flow conditions: Cyrene/H$_2$O solution: 0.03 mL min^{-1}, H$_2$ gas: 20 mL min^{-1}.
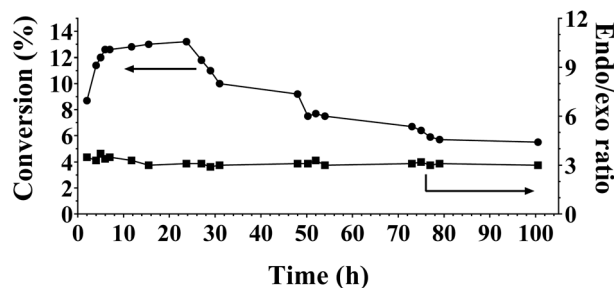
Fig. 8 Activity of reduced Cu8/MgAlOx-**HP** in flow (353 K, 60 bar H_2, 5 wt% Cyrene in H_2O). Flow conditions: Cyrene/H_2O solution: 0.03 mL min^{-1}, H_2 gas: 20 mL min^{-1}.

feed from 1 to 5 wt% for up to 25 h (Fig. 8). The maximal TOF of 0.011 s^{-1} (353 K) is similar to the one obtained when using a 1 wt% Cyrene feed (0.013 s^{-1} at 353 K). Longer reaction times do however show a progressive deactivation (Fig. 8). As stable activity was observed when using a 1 wt% Cyrene in H_2O feed (pH 4.25) (Fig. 7), this behaviour is attributed to the constant exposure of the catalytic bed to a Cyrene/H_2O feed (5 wt%) with a lower pH of 3.75 (see also Fig. 5C). It is noteworthy, however, that ultimately a stabilization of the catalytic activity occurs with a constant 5.5% conversion (TOF 0.005 s^{-1} at 353 K) (Fig. 8). The number of turnovers for the reaction shown in Fig. 8 was 2654 mol Cyrene per mol Cu. A small amount of Cu and Mg leaching was found with 5–10 ppb Cu and 30 ppm Mg in the reactor effluent.

Reduced Cu8/MgAlO$_x$-**LP** was also found to be stable in flow reactor studies (1 wt% Cyrene feed) yet at a lower activity than Cu8/MgAlO$_x$-**HP**, their respective turnover frequencies being 0.0105 s^{-1} (353 K) and 0.0130 s^{-1} (353 K). This result is in line with the previously discussed batch experiments (see Fig. 2). This result also indicates that meso/macroporosity positively influences the activity level of the catalyst but is not crucial to its stability. Also, the use of (expensive) pluronic in the synthesis method of the layered double hydroxides is not a necessity. With Cu8/MgAlOx-**LP** Mg leaching was determined at 5 ppm and no evidence of Cu leaching could be established. The turnover frequency achieved with Cu8/MgAlO$_x$-**HP** [0.013 s^{-1}, 353 K] is half that obtained using 0.4 wt% Pd/Al$_2$O$_3$ [0.025 s^{-1}, 353 K]. However, while the Cu8/MgAlO$_x$-**HP** catalyst shows a stable activity, the activity of 0.4 wt% Pd/Al$_2$O$_3$ decreases with time-on-stream (Fig. 3S†). The latter decrease in activity does not relate to Pd leaching.

Comparison flow *vs*. batch reactions

The difference between the flow and batch reactor studies using 5 wt% Cyrene in water manifests itself at different levels:

(1) While Mg is progressively lost under flow operation, the situation is different when the reaction is run in batch. In batch, any leached Mg remains in the reactor and could potentially influence the speciation of copper and/or the reaction. As such, it is found that the TOF of Cu8/AlMgO$_x$-**HP** when operated in batch [0.04 s^{-1} at 353 K for a 5 wt% Cyrene/H_2O feed]

is higher than the one attained in flow [at 353 K: 0.013 s^{-1} for a 1 wt% Cyrene/H_2O feed and 0.011 s^{-1} for a 5 wt% Cyrene/H_2O feed].

(2) At a concentration of 5 wt% Cyrene in water, the pH of the reaction mixture is ~3.75. In a flow reactor set-up, this value is the pH that the catalyst bed will be exposed to continuously – affecting the entire catalyst bed over time. In contrast, in a batch reactor this pH will gradually increase as Cyrene present in the reaction mixture converts into non-acidic levoglucosanol. With Cyrene being in equilibrium with its acidic geminal diol, any conversion of Cyrene into levoglucosanol also means a decrease of the concentration of Cyrene's geminal diol and hence a gradual increase of the pH in the batch reaction mixture.

(3) At a concentration of 1 wt% Cyrene in water, the pH of the reaction mixture is ~4.25. As shown in Fig. 7, under these conditions the Cu8/AlMgO$_x$-**HP**/**LP** catalysts are less affected, both showing constant activity.

(4) We also note that hydrotalcite is a basic support and in batch reactor studies it will have a larger additional effect on the pH (catalyst exposure to 5 mL of 5 wt% Cyrene in water)
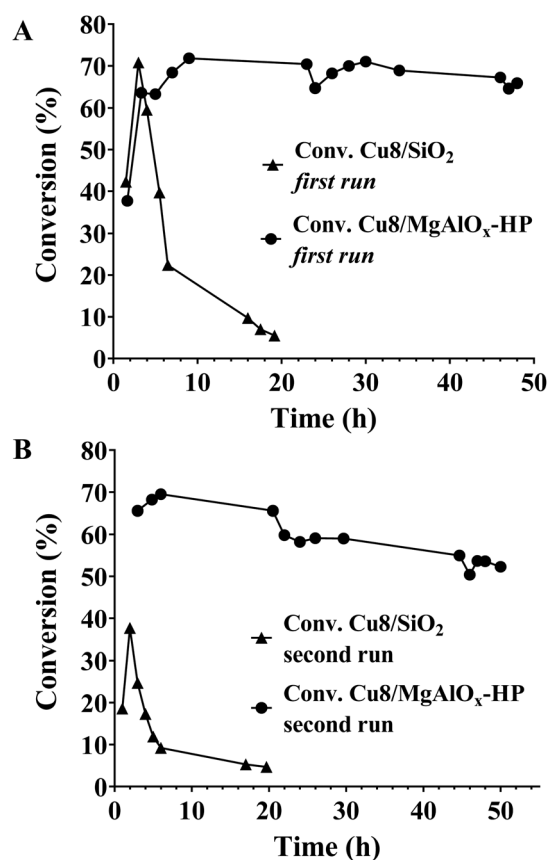

Fig. 9 (A) 1st run flow Cyrene/LGOL hydrogenation reaction using an oxidized/reduced Cu8/MgAlO$_x$-**HP** and an oxidized/reduced Cu8/SiO$_2$ material (B) 2nd run flow Cyrene/LGOL hydrogenation reaction using Cu8/MgAlO$_x$-**HP** and Cu8/SiO$_2$. Reaction conditions: 353 K, 60 bar H_2, 1 wt% Cyrene in H_2O. Flow conditions: Cyrene/H_2O solution: 0.03 mL min^{-1}, H_2 gas: 20 mL min^{-1}.

than in a flow setting (catalyst exposure to 100–250 mL of 1–5 wt% Cyrene in water).

Reference reaction

The catalytic performance in the flow mode of oxidized/reduced Cu8/MgAlO$_x$-**HP** in the Cyrene/LGOL hydrogenation reaction was compared to oxidized/reduced Cu8/SiO$_2$ as a reference catalyst. As can be seen from Fig. 9A, the first run with Cu8/SiO$_2$ showed initially a similar activity to Cu8/MgAlO$_x$-**HP** which then rapidly decreases. Re-oxidation and re-reduction of the spent Cu8/SiO$_2$ catalyst showed a further decrease of the catalytic activity (Fig. 9A ↔ 9B). A Cu8/SiO$_2$ catalyst that has only been subjected to reduction displays a similar behaviour, as shown in Fig. 4S.† Irrespective the pre-treatment, the deactivation of Cu8/SiO$_2$ is not due to Cu leaching.

Conclusion

We have demonstrated that Cu supported on hydrotalcite can attain a high and stable catalytic activity for hydrogenation of Cyrene, and this behaviour is independent of the exact pre-treatment conditions, but with a preference to re-reduction over additional oxidation/reduction cycles. Performance of the catalyst in flow reactor studies is distinctly different from batch operation, with higher TOF numbers for batch operation. The heterogeneous Cu-catalysts do not undergo leaching of Cu, which is a rare feature in the absence of special nanoparticle coatings (e.g. ALD). Leaching of Mg was observed, which could be linked to the presence of the geminal diol functionality of Cyrene, an acidic species. TEM imaging revealed further that the Cu particle size distribution remains unchanged before and after reaction. Given the dilute aqueous reaction media (1–5 wt% Cyrene in water), direct isolation of levoglucosanol is preferentially achieved by extraction with benign bio-based solvents, such as 2-methyltetrahydrofuran.[28] However, as presently levoglucosanol has no known applications, its main potential lies in its further conversion to added-value products, such as hexane-1,2,5,6-tetrol, THFDM; 1,2,6-hexanetriol and 1,6-hexanediol (Fig. 1). As the formation of the latter compounds from levoglucosanol requires the presence of an aqueous medium, no immediate need exists to isolate levoglucosanol. The presence of limited quantities of Mg (ppm) is not expected to influence the isolation procedures involved for production of levoglucosanol or any of its derivatives. Future work will involve the evaluation of the Cu8/MgAlO$_x$-**HP** catalyst towards the hydrogenation of a range of carbonyl-containing substrates and a full elucidation of the catalytic cycle.

Conflicts of interest

There are no conflicts to declare.

Acknowledgements

References

1 R. Schlogl, *Angew. Chem., Int. Ed.*, 2015, **54**, 3465–3520.

2 J. W. Medlin and M. M. Montemore, *Nat. Chem.*, 2015, **7**, 378–380.

3 Y. C. Lin and G. W. Huber, *Energy Environ. Sci.*, 2009, **2**, 68–80.

4 B. N. Kuznetsov, N. V. Chesnokov, O. V. Yatsenkova and V. I. Sharypov, *Russ. Chem. Bull.*, 2013, **62**, 1493–1502.

5 Critical raw materials for the EU, https://ec.europa.eu/growth/tools-databases/eip-raw-materials/en/system/files/ged/79%20report-b_en.pdf, (accessed 10/09/2018).

6 L. Leyssens, B. Vinck, C. Van Der Straeten, F. Wuyts and L. Maes, *Toxicology*, 2017, **387**, 43–56.

7 K. K. Das, S. N. Das and S. A. Dhundasi, *Indian J. Med. Res.*, 2008, **128**, 412–425.

8 J. C. Lee, D. H. K. Jackson, T. Li, R. E. Winans, J. A. Dumesic, T. F. Kuech and G. W. Huber, *Energy Environ. Sci.*, 2014, **7**, 1657–1660.

9 F. Holmes, The World's Cobalt Supply is in Jeopardy, *Forbes*, 2018.

10 M. B. Gawande, A. Goswami, F. X. Felpin, T. Asefa, X. X. Huang, R. Silva, X. X. Zou, R. Zboril and R. S. Varma, *Chem. Rev.*, 2016, **116**, 3722–3811.

11 R. P. Ye, L. Lin, Q. H. Li, Z. F. Zhou, T. T. Wang, C. K. Russell, H. Adidharma, Z. H. Xu, Y. G. Yao and M. H. Fan, *Catal. Sci. Technol.*, 2018, **8**, 3428–3449.

12 N. Kaeffer, K. Larmier, A. Fedorov and C. Coperet, *J. Catal.*, 2018, **364**, 437–445.

13 T. Subramanian and K. Pitchumani, *Catal. Sci. Technol.*, 2012, **2**, 296–300.

14 R. Y. Fan, C. Chen, M. M. Han, W. B. Gong, H. M. Zhang, Y. X. Zhang, H. J. Zhao and G. Z. Wang, *Small*, 2018, **14**, 1801953.

15 F. Heroguel, B. P. Le Monnier, K. S. Brown, J. C. Siu and J. S. Luterbacher, *Appl. Catal., B*, 2017, **218**, 643–649.

16 R. Mariscal, P. Maireles-Torres, M. Ojeda, I. Sadaba and M. L. Granados, *Energy Environ. Sci.*, 2016, **9**, 1144–1189.

17 M. De Bruyn, J. Fan, V. L. Budarin, D. J. Macquarrie, L. D. Gomez, R. Simister, T. J. Farmer, W. D. Raverty, S. J. McQueen-Mason and J. H. Clark, *Energy Environ. Sci.*, 2016, **9**, 2571–2574.

18 J. Y. He, M. J. Liu, K. F. Huang, T. W. Walker, C. T. Maravelias, J. A. Dumesic and G. W. Huber, *Green Chem.*, 2017, **19**, 3642–3653.

19 G. R. Court, C. H. Lawrence, W. D. Raverty and A. J. Duncan, *Method for converting lignocellulosic materials into useful chemicals*, 2011/000030A1, 2011.

20 J. Y. He, S. P. Burt, M. Ball, D. T. Zhao, I. Hermans, J. A. Dumesic and G. W. Huber, *ACS Catal.*, 2018, **8**, 1427–1439.

21 S. H. Krishna, D. J. McClelland, Q. A. Rashke, J. A. Dumesic and G. W. Huber, *Green Chem.*, 2017, **19**, 1278–1285.

22 A. M. Allgeier, W. I. N. De Silva, E. Korovessi, C. A. Menning, J. C. Ritter, S. K. Sengupta and D. R. Corbin, *Process for preparing 1, 6-hexanediol*, EP2797866(A1), 2014.

23 S. H. Krishna, M. De bruyn, Z. R. Schmidt, B. M. Weckhuysen, J. A. Dumesic and G. W. Huber, *Green Chem.*, 2018, **20**, 4557–4565.

24 D. D. Petrolini, E. A. Urquieta-Gonzalez, S. H. Pulcinelli, C. V. Santilli and L. Martins, *Microporous Mesoporous Mater.*, 2017, **240**, 149–158.

25 M. De bruyn, A. Misefari, S. Shimizu, H. Fish, M. Cockett, A. J. Hunt, H. Hofstetter, B. M. Weckhuysen, J. H. Clark and D. J. Macquarrie, *ACS Sustainable Chem. Eng.*, 2019, **7**(8), 7878–7883.

26 I. Delidovich and R. Palkovits, *Catal. Sci. Technol.*, 2014, **4**, 4322–4329.

27 C. Y. Hu, K. M. Shih and J. O. Leckie, *J. Hazard. Mater.*, 2010, **181**, 399–404.

28 D. F. Aycock, *Org. Process Res. Dev.*, 2007, **11**, 156–159.